Title
Strong zonal winds from thermal convection in a rotating spherical shell

Journal
Geophysical Research Letters, 28(13)

ISSN
0094-8276

Authors
Aurnou, Jonathan M
Olson, Peter L

Publication Date
2001-07-01

DOI
10.1029/2000gl012474

Peer reviewed

GEOPHYSICAL RESEARCH LETTERS, VOL. 28, NO. 13, PAGES 2557-2559, JULY 1, 2001

Strong zonal winds from thermal convection in a rotating spherical shell

Jonathan M. Aurnou

Department of Terrestrial Magnetism, Carnegie Institution of Washington, Washington, DC

Peter L. Olson

Department of Earth and Planetary Sciences, Johns Hopkins University, Baltimore, MD

Abstract. Zonal wind (ZW) generation by thermal convection in rotating spherical shells is studied using numerical calculations. Strong ZW accompany quasi-geostrophic, high Rayleigh number convection in shells with stress-free boundaries. In a thin shell (radius ratio 0.75) with stress-free boundaries, nearly 90% of the total kinetic energy is contained in the ZW at Rayleigh number 10^6 and Taylor number 4.4×10^7. The same parameters in a thicker shell produce weaker convection and weaker ZW. Rigid boundaries reduce the kinetic energy in the ZW to less than 20% of the total. The ZW are eastward (prograde) in the equatorial region and westward at higher latitudes, and are driven by Reynolds stresses associated with the convection. Episodes with strong ZW alternate with episodes of strong convection. Although far from the dynamical regime of Jupiter and Saturn, our results support the interpretation that the prograde equatorial jets on these planets originate from deep convection.

Introduction

The dominant circulation on the giant planets is a system of zonal winds [*Gierasch and Conrath*, 1993; *Dowling*, 1995]. Both Jupiter and Saturn have strong eastward jets in the equatorial region, and a pattern of alternating east-west winds at higher latitudes [*Beebe*, 1994]. Despite the wealth of information on the giant planets, the origin of these zonal jets remains uncertain.

Zonal winds (ZW) refer to the axisymmetric part of the azimuthal (east-west) fluid velocity. Observations indicate that the ZW on Jupiter extend to significant depths, and are related to atmospheric convection. The Galileo probe measured wind speeds of 170 m/s down to ∼125 km beneath the cloud tops [*Atkinson et al.*, 1998]. Since the surface heat loss is nearly twice that received from solar insolation [*Hanel et al.*, 1981; 1983], convective heat transfer is important in the deep atmosphere of each planet [*Stevenson*, 1982]. However, the depth of the convection is unknown. Here we assume it occupies the outer 25% of Jupiter, where models indicate the molecular-metallic hydrogen phase transition and changes in hydrogen-helium ratios occur [*Guillot*, 1999].

Earlier studies of rotating spherical convection produced weaker ZW with low Rossby number values [*Zhang*, 1992; *Sun et al.*, 1993; *Manneville and Olson*, 1996]. Recent calculations by *Christensen* [2001] show that convection can produce strong ZW if the convection is fully developed and the ratio of the Rayleigh to Taylor numbers is in a certain range.

Paper number 2000GL000000.
0094-8276/01/2000GL000000$05.00

Numerical Model

We compare the ZW generation in numerical models of 3D time-dependent thermal convection in a rotating Boussinesq fluid. Two spherical geometries are considered. The first is a thin shell, with an inner/outer radius ratio $r_i/r_o = 0.75$; the second is a thicker shell with $r_i/r_o = 0.35$. For each geometry, two mechanical boundary conditions are considered: (i) zero-slip (rigid) at r_i and r_o, and (ii) zero-stress (free) at the same surfaces. In all other respects, the calculations are the same. The shell boundaries are isothermal and gravity varies linearly with radius. The governing dimensionless parameters are the Taylor number, $Ta = 4\Omega^2 D^4/\nu^2 = 4.4\times10^7$, the Rayleigh number, $Ra = \alpha g \Delta T D^3/\nu\kappa = 10^6$, and the Prandtl number, $Pr = \nu/\kappa = 1$. Here α is the thermal expansion coefficient, g is the gravitational acceleration at r_o, Ω is the angular velocity of rotation, ν is the kinematic viscosity, κ is the thermal diffusivity, $D = r_o$-r_i is the shell thickness, and ΔT is the temperature difference across the shell. The Rayleigh number is roughly six times critical in all four cases [*Zhang and Jones*, 1993]. No hyperdiffusivities are used in these calculations. Dimensionless fluid velocities are given in Rossby number $Ro = u/2\Omega D$ units, where u is the ZW velocity. Dimensionless heat flux is expressed as the Nusselt number $Nu = FD/k\Delta T$, where F is the total heat flux and k is the thermal conductivity. Time is measured in viscous diffusive time scales D^2/ν. The numerical technique is described in *Christensen et al.* [1999]. In the radial direction we use Chebyshev polynomials with 25 nodes concentrated near the boundaries. We use 144 and 288 grid points in colatitude and longitude, respectively, and truncate at spherical harmonic degree and order 96. In order to make sufficiently long calculations (one diffusion time) we impose six-fold longitudinal symmetry on the solutions. Each calculation is initialized with a thermal perturbation.

Flow Patterns

Figure 1 shows instantaneous patterns of velocity and heat flow from the four cases. Results from the thin shell calculation with stress-free boundaries are shown in Figure 1*a-c*. The convection planform consists of an array of columnar cells, sheared into a pinwheel pattern by the strong zonal flow. The azimuthal wavenumber of the convection

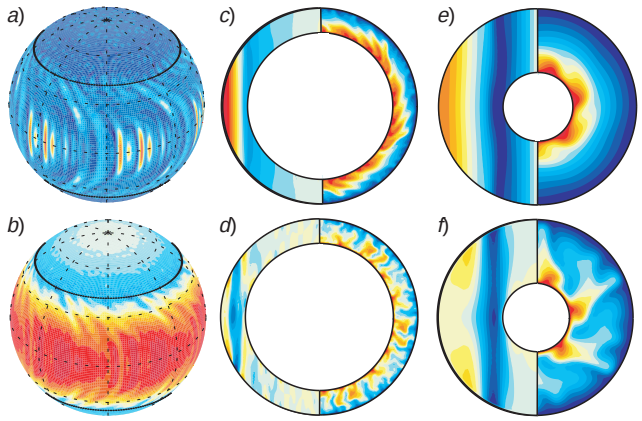

Figure 1. Thermal convection in rotating spherical shells at $Ta = 4.4\times10^7$, $Ra = 10^6$, and $Pr = 1$. First column: outer surface heat flux (a) and azimuthal velocity pattern (b) for the thin shell ($r_i/r_o = 0.75$) with stress-free boundaries. Second column: thin shell sections with free (c) and rigid boundaries (d). Third column: thick shell sections with free (e) and rigid boundaries (f). In c-f, left halves show contours of zonal azimuthal velocity. Right halves show contours of temperature in the equatorial plane. Contours from blue (minimum) to red (maximum).

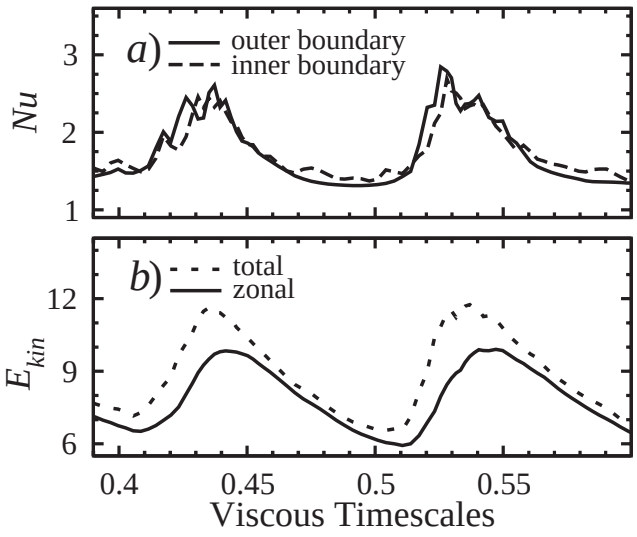

Figure 3. Time series of convective oscillations in the stress-free thin shell case. a) average Nusselt number on the boundaries; b) kinetic energy of the total and zonal velocity fields (dimensionless, normalized by 10^3).

columns is $m \approx 30$, in agreement with theory for the onset of convection in a rotating annulus [*Tilgner and Busse*, 1997]. The zonal flow is basically geostrophic (invariant along the direction of the rotation axis). It is predominantly eastward (prograde) outside of the tangent cylinder of the inner spherical boundary, and reaches its maximum speed at the equator. At higher latitudes, the zonal flow is westward. Zonal flow vanishes toward the poles, where the convection appears to be near critical.

Figure 1d shows results from the rigid thin shell. A very weak large-scale zonal flow is generated in this case. Along the inner equator, the convection has an $m \approx 24$ azimuthal wavenumber, while the characteristic wavenumber is $m \approx 48$ along the outer equator. A similar radial increase in wavenumber has been seen in experiments by *Sumita and Olson* [2000], caused by plumes dividing as they meander across the shell.

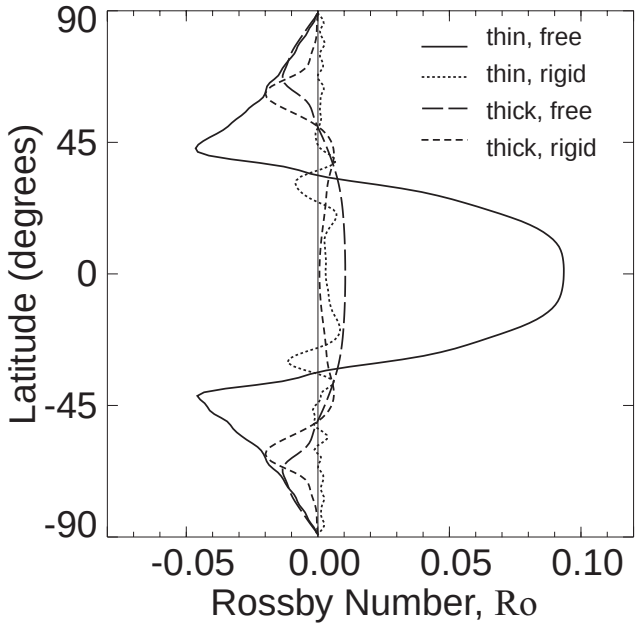

Figure 2. Zonally-averaged azimuthal velocity versus latitude. Velocity is expressed in Rossby number $Ro = u/2\Omega D$ units.

Figure 1e shows results from the thick shell with free boundaries. These conditions permit a relatively strong zonal flow. Here the zonal flow at the outer boundary is prograde below latitude 50^o and retrograde above 50^o in each hemisphere. This flow pattern imparts a spiral structure to the convection planform, similar to results by *Zhang* [1992]. In the thick shell the characteristic azimuthal wavenumber is $m = 6$. For comparison, the theory of *Tilgner and Busse* [1997] predicts $m \sim 5$ at convective onset for the same parameters.

Figure 1f shows results from the thick shell with rigid boundaries. This case produces a weak retrograde zonal flow near the tangent cylinder and a weak thermal wind near the outer boundary. The convection consists of an array of six columnar plumes that extend from the tangent cylinder to the outer boundary. Here the plumes show some division, but it is not complete.

Figure 2 shows the variation of zonal velocity with latitude near the outer boundary for the four cases. The ratio of zonal velocities versus convective velocities is about 10 in the stress-free cases and about 1 in the rigid boundary cases. In the stress-free thin shell case, the maximum ZW occurs in the center of the equatorial jet, where $Ro \simeq 0.1$. A similar ZW pattern was found by *Zhang* [1992] in a low Prandtl number fluid. The ZW in the other cases are substantially weaker, with $Ro \simeq 0.01$.

Time averages of the Nusselt number on the outer boundary Nu, the total kinetic energy E_{kin}, and the kinetic energy in the zonal flow divided by the total kinetic energy e_{zt} are given in Table 1. There is an inverse correlation between the fraction of the kinetic energy in the ZW and heat transport by the convection. The total kinetic energy is more sensitive to shell thickness than to mechanical boundary conditions.

Table 1. Time averages from the calculations.

Shell	Nu	E_{kin}	e_{zt}
thin, free	1.82 ± 0.44	9.43 ± 1.52	0.89
thin, rigid	3.43 ± 0.22	3.62 ± 0.49	0.04
thick, free	1.22 ± 0.05	0.67 ± 0.20	0.75
thick, rigid	1.78 ± 0.14	0.81 ± 0.25	0.16

Mechanics of Zonal Wind Generation

The calculations with strong zonal flows show oscillations in ZW speed and intensity of convection, which illustrate how the ZW are sustained. Figure 3 shows time series from the stress-free thin shell case. Upward spikes in the Nu coincide with increases in the E_{kin} total and drops in e_{zt}. The sudden increases in E_{kin} total and Nu correspond to breakout events, where the convection intensifies. Prior to these events, the ZW are weak and the plumes are developing. As the plumes traverse the shell, they develop a prograde tilt, and induce azimuthal Reynolds stresses, which accelerate the ZW. The intensified ZW then shear out the plumes, tending to suppress the convection. This leads to a decrease in the Reynolds stresses and the ZW decelerate. The convection then redevelops, and the cycle repeats.

ZW are generated by Reynolds stresses, by thermal winds, or by both mechanisms jointly, and are resisted by viscous stresses. Reynolds stresses produce nearly geostrophic flows (Fig. 1*c*, 1*e*), whereas thermal winds contain shear in the axial direction (Fig. 1*d*, 1*f*). In our calculations, convection within the tangent cylinder is weak or non-existent. Convection tends to occur at lower Ra outside the tangent cylinder, compared to inside [*Tilgner and Busse*, 1997; *Christensen et al.*, 1999]. *Christensen* [2001] finds, at higher Ra, zonal flows outside the tangent cylinder similar to our stress-free cases. He also finds strong convection excited within the tangent cylinder, and a pattern of weaker, alternating ZW there.

Discussion

These calculations are not directly applicable to the general circulation in the interiors of the giant planets, because the Ra and Ta are far smaller than planetary values, and because we do not include a stratified uppermost atmosphere or electrical conductivity. It has been argued that stratification and hydromagnetic effects may also be important in this part of the atmosphere [*Zhang and Schubert*, 2000; *Kirk and Stevenson*, 1987]. Even so, we have identified conditions that promote prograde equatorial jets by convection in a deep planetary shell, which may have significance for the giant planets. First, convection with stress-free boundaries results in a strong prograde equatorial jet flanked by strong retrograde jets. The ZW produced by convective Reynolds stresses contain most of the kinetic energy in the flow. Second, the velocity of the ZW is higher in thin shells, because the strongly tilted convection columns are better organized than in thicker shells. In our calculations the equatorial jet has a Rossby number comparable to that inferred for the equatorial jet on Jupiter, even though our Ra and Ta are unrealistically low. Calculations at higher Ra and Ta are necessary to establish an asymptotic scaling law for the ZW. *Christensen* [2001] has proposed one such law at moderate Ra and Ta values, but additional calculations at larger values of the parameters are still needed.

Acknowledgments. We thank G. Glatzmaier for making his convection code available to us and U. Christensen for sharing his results in advance of publication. This research was supported by the NSF Geophysics Program and NASA grants NAG5-4077 and NAG5-10165.

References

Atkinson, D.H., J.B. Pollack and A. Seiff, The Galileo Probe Doppler Wind Experiment: Measurement of the deep zonal winds on Jupiter, *J. Geophys. Res., 103*, 22911-22928, 1998.

Christensen, U.R., A numerical model of zonal flow on the major planets driven by deep convection, *Geophys. Res. Lett.*, in press.

Christensen, U.R., P.L. Olson and G.A. Glatzmaier, Numerical modelling of the geodynamo: A systematic parameter study, *Geophys. J. Int.*, *138*, 393-409, 1999.

Dowling, T.E., Dynamics of the Jovian Atmosphere, *Ann. Rev. Fluid Mech.*, *27*, 293-334, 1995.

Gierasch, P.J. and B.J. Conrath, Dynamics of the atmospheres of the outer planets: post-Voyager measurement objectives, *J. Geophys. Res.*, *98*, 5459-5469, 1993.

Guillot, T., Interiors of giant planets inside and outside the solar system, *Science*, *286*, 72-77, 1999.

Hanel, R.A., et al., Albedo, internal heat, and energy balance of Jupiter: Preliminary results of the Voyager infrared investigation, *J. Geophys. Res., 86*, 8705-8712, 1981.

Hanel, R.A., et al., Albedo, internal heat, and energy balance of Saturn, *Icarus*, *53*, 262-285, 1983.

Kirk, R.L. and D.J. Stevenson, Hydromagnetic constraints on deep zonal flow in the giant planets, *Astrophys. J.*, *316*, 836-846, 1987.

Manneville, J.B. and P.L. Olson, Banded convection in rotating fluid spheres and the circulation of the Jovian atmosphere, *Icarus*, *122*, 242-350, 1996.

Sumita, I. and P. Olson, Laboratory experiments on high Rayleigh number thermal convection in a rapidly rotating spherical shell, *Phys. Earth. Planet. Inter.*, *117*, 153-170, 2000.

Sun, Z.P., G. Schubert and G.A. Glatzmaier, Banded surface flow maintained by convection in a model of the rapidly rotating giant planets, *Science*, *260*, 661-664, 1993.

Tilgner, A. and F.H. Busse, Finite-amplitude convection in rotating spherical shells, *J. Fluid Mech.*, *332*, 359-376, 1997.

Zhang, K., Spiralling columnar convection in rapidly rotating spherical fluid shells, *J. Fluid Mech.*, *236*, 535-556, 1992.

Zhang, K. and C.A. Jones, The influence of Ekman boundary layers on rotating convection, *Geophys. Astrophys. Fluid Dyn.*, *71*, 145-162, 1993.

Zhang, K. and G. Schubert, Teleconvection: Remotely driven thermal convection in rotating stratified spherical layers, *Science*, *290*, 1944-1947, 2000.

J. M. Aurnou, Department of Terrestrial Magnetism, Carnegie Institution of Washington, Washington, DC 20015. (e-mail:jona@dtm.ciw.edu)

P. L. Olson, Department of Earth and Planetary Sciences, Johns Hopkins University, Baltimore, MD 21218. (e-mail:olson@jhu.edu)

(Received October 10, 2000; revised January 10, 2001;
accepted March 7, 2001.)